Originally published as:

Research paper

Berthierine formation in reservoir rocks from the Siri oilfield (Danish North Sea) as result of fluid–rock interactions: Part III. Determining mineral stability and CO_2-sequestering capacity of glauconitic sandstones

Yunjiao Fu [a,1], Wolfgang van Berk [b,*], Hans-Martin Schulz [a], Nana Mu [a]

[a] Helmhotz Centre Potsdam–GFZ German Research Centre for Geosciences, Section 4.3 Organic Geochemistry, Telegrafenberg, D-14473 Potsdam, Germany
[b] Clausthal University of Technology, Department of Hydrogeology, Leibnizstraße 10, D-38678 Clausthal-Zellerfeld, Germany

ABSTRACT

Berthierine was proven as one of the most important products of glauconite alteration in the Siri oilfield (Danish North Sea). However, there is an ongoing debate regarding the main product of glauconite dissolution: siderite, berthierine, or berthierine as a precursor of siderite and/or magnesium-bearing carbonate. In order to investigate the consequences of glauconite dissolution in view of thermodynamic admissibility and the resulting CO_2-sequestering capacity, a hydrogeochemical model, which is based on thermodynamics of chemical equilibrium, was developed. Calculating various modeling scenarios helps to conclude on the pH-E_H conditions of glauconite dissolution as well as of berthierine formation and dissolution in generic, aqueous systems under elevated temperature-pressure conditions.

Our modeling results highlight that carbonate formation cannot be triggered exclusively by CO_2 addition into glauconitic sandstones. The injection of pure CO_2 into glauconitic sandstones leads to acidic and anoxic oxidizing conditions under which glauconite remains stable. To intensify glauconite alteration by CO_2 injection, glauconitic sandstones have to be in contact with degradable organic matter, or, alternatively, reducing agents have to be co-injected with CO_2. Sufficient electron transfer to ferric iron bound in glauconite is the ultimate control for intense glauconite alteration and for subsequent berthierine precipitation.

Once formed, berthierine remains stable over a broad pH range and is not transformed to any carbonate under reducing conditions. Thus, CO_2 injection into glauconitic sandstones under reducing conditions mainly leads to formation of berthierine instead of iron- and magnesium-carbonates. However, hydrogeochemical conditions in the subsurface can affect CO_2 sequestration via glauconite dissolution and the resulting carbonate formation, including the pH-E_H conditions, the chemical composition of glauconite, and the overall mineralogical composition of glauconitic sandstones.

1. Introduction

Glauconite, which belongs to the mica group, is rich in ferric iron and contains small amounts of ferrous iron (Amouric and Parron, 1985; Mackenzie et al., 1988, and references therein). Apart from its high iron content, glauconite also contains magnesium as a major component. Therefore, glauconitic sandstones are often regarded as potential CO_2 storage sites via carbonate precipitation (e.g., Gunter et al., 2000). In order to investigate whether glauconitic sandstones can efficiently trap CO_2 in the subsurface, the sandstone aquifer of the Alberta Sedimentary Basin in Canada, which contains 5 wt.-% of glauconite, is often referred to as a natural laboratory in many studies (e.g., Gunter et al., 1997, 2000; Pruess et al., 2002; Kumar et al., 2004; Xu et al., 2004; Bacon and Murphy, 2011). Kumar et al. (2004) considered three aqueous reactions and five mineral reactions in their modeling approach in order to investigate the CO_2-sequestering capacity of the glauconitic sandstones of the Alberta Sedimentary Basin. They stated that CO_2 sequestration can be achieved via precipitation of calcite and

* Corresponding author. Tel.: +49 5323 72 2234; fax: +49 5323 72 2903.
E-mail address: wolfgang.van.berk@tu-clausthal.de (W. van Berk).
[1] Present address: Clausthal University of Technology, Department of Hydrogeology, Leibnizstraße 10, D-38678 Clausthal-Zellerfeld, Germany.

siderite. Gunter et al. (1997, 2000) substituted Mg-bearing glauconite, in which Fe(III) dominates, by Mg-free annite that exclusively contains ferrous iron. In their study, CO_2-trapping was efficiently achieved via annite dissolution and siderite precipitation. However, such a substitution of glauconite by annite is clearly inappropriate due to the different hydrogeochemical behavior between $Fe^{3+}_{(aq)}$ and $Fe^{2+}_{(aq)}$ species. The modeling approaches presented by Pruess et al. (2002) and Xu et al. (2004) also substituted glauconite by annite, but assumed the presence of oxidizable organic matter in the sandstones to generically bypass the transformation of ferric iron bound in glauconite to ferrous iron in annite. Nevertheless, these approaches are incapable of correctly predicting the CO_2-sequestering capacity in glauconite-bearing sandstones. The reason for this is that annite is free of Mg, and, therefore, such a replacement could bypass the potential formation of any Mg-bearing mineral, for instance, My-bearing silicates or Mg-bearing carbonates. Bacon and Murphy (2011) suggested that CO_2 sequestration in the glauconitic sandstone of the Alberta Sedimentary Basin mainly occurs via precipitation of dolomite and siderite. However, there are also other studies that reported a limited CO_2 trapping-capacity of glauconitic sandstones. For instance, Humez et al. (2011) suggested that injection of pure CO_2 into glauconitic sandstones may lead to a low pH and even to dissolution of primary calcite.

The abovementioned studies offer opposite views about CO_2 sequestration in glauconitic sandstones. Several of them considered selected and isolated hydrogeochemical reactions, and excluded the potential formation of any secondary Fe-und Mg-bearing silicate mineral, for instance, berthierine ((Fe^{2+},Mg,Al)$_{2-3}$(Si,Al)$_2O_5$(OH)$_4$). A combination of analytical investigations and hydrogeochemical modeling highlights that berthierine formation acts as one of the most important diagenetic processes of glauconite alteration in the reservoir rocks of the Siri oilfield (Danish North Sea; Fu et al., 2015). In addition, berthierine co-exists with altered glauconite in the Nullawarre Greensand containing organic lamellae and bone fragments (in southeastern Australia; Boyd et al., 2004). Berthierine forms only under reducing conditions and is transformed to other minerals in the presence of molecular oxygen (Sheldon and Retallack, 2002; Rivard et al., 2013). The exclusion or neglect of potential berthierine formation in glauconitic sandstones could lead to a strong overestimation of the calculated CO_2-sequestering capacity. Although siderite formation was proven in the glauconitic reservoir rocks of the Siri field, it is not a product of glauconite alteration (Fu et al., 2015). In contrast, the calculated results of several modeling approaches stated that siderite newly forms in glauconitic sandstones due to CO_2 injection (e.g., Gunter et al., 2000; Xu et al., 2004).

In summary, a debate about the CO_2-sequestration in glauconitic sandstones focuses on which secondary Fe-bearing mineral (siderite or berthierine) acts as the thermodynamically stable product of glauconite alteration. Such debate leads to the following concrete questions:

(1) under which hydrogeochemical conditions does glauconite dissolve (especially regarding the pH-E_H conditions)?
(2) which iron-bearing minerals are concurrently precipitated as a result of glauconite dissolution, berthierine or CO_2-sequestering, Fe- and/or Mg-bearing carbonates?
(3) if berthierine newly forms, can it further be converted to Fe- and/or Mg-bearing carbonates?
(4) can CO_2 sequestration be achieved via glauconite dissolution and concurrent carbonate formation?
(5) if so, which factors can influence the CO_2-sequestering capacity of glauconitic sandstones?

Gaus et al. (2005) stated that CO_2-sequestration via water-rock reactions can be sluggish and the sequestrating capacity can be limited due to kinetic inhibition of several reactions involved in the CO_2-water-rock web. However, kinetic rates can limit the progress and the mass transfer of reactions, only when such reactions are thermodynamically admissible. The presented study aims to answer the aforementioned questions from a thermodynamic point of view and therefore presents a hydrogeochemical model based on thermodynamics of chemical equilibrium. This model considers all chemical processes that potentially proceed as a result of glauconite alteration. Varying hydrogeochemical conditions of aqueous solutions in different modeling scenarios shall illustrate specific pH-E_H conditions of glauconite dissolution as well as of berthierine formation and dissolution. Besides relevance for pure geoscience, the gained results offer a broad spectrum for further technical applications. Our modeling results could help to conclude on the CO_2-sequestering capacity of glauconitic sandstones, to identify its influencing factors, and, consequently, to improve CO_2 sequestration. Moreover, an elucidation of such physicochemical factors can be used to consider berthierine dissolution in order to improve hydrocarbon production, because berthierine formation can deteriorate reservoir permeability (e.g., in the Siri field; Stokkendal et al., 2009).

2. Hydrogeochemical modeling concept

The developed hydrogeochemical model uses a closed, isothermal, iso-chemical, generic reactor within which a state of chemical equilibrium among aqueous solutions, mineral phases and a free gas phase is reached. By means of hydrogeochemical modeling, Fu et al. (2012, 2013) demonstrated that several water-–rock–gas reactions rapidly achieve equilibrium conditions at reservoir conditions. The presented study aims to investigate whether siderite or berthierine is the thermodynamically stable product of glauconite alteration resulting from CO_2 injection. Thus, no kinetic aspect is integrated into this hydrogeochemical zero-dimensional (batch) modeling approach.

The reactor is filled with one liter of pore water and generically considers 1.0 mol of glauconite or berthierine as the single primary mineral which is initially present in the reactor (Table 1). A 1.5 molal NaCl solution is used as the pore water of the reactor and is exposed to temperature-pressure conditions of 78 °C and 230 atm which also prevail in the Siri field. This aims to compare the calculated results of this presented study with the observed and the calculated results of the diagenetic features in the glauconitic sandstones of the Siri field (Fu et al., 2015). A series of modeling scenarios were calculated to investigate the pH-E_H conditions of glauconite dissolution, as well as of berthierine formation and dissolution (Table 1). These scenarios cover a broad range of pH-E_H conditions that were conceptually designed by stepwise addition of different reactants (CO_2, CH_4, or O_2) triggering proton- and electron
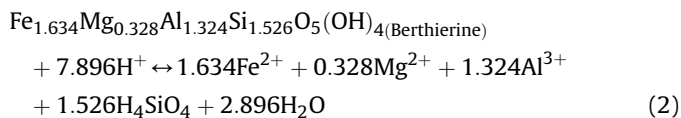
Table 1
Modeling scenarios.

	Primary mineral assemblage	Added reactants	Redox conditions
Gl-CO_2	Glauconite[a]	CO_2	Oxidizing
Gl-CH_4	Glauconite	CH_4	Reducing
Gl-CO_2 + CH_4	Glauconite	CO_2, CH_4	Reducing
Gl2-CO_2 + CH_4	Glauconite2[b]	CO_2, CH_4	Reducing
Be-CO_2	Berthierine[c]	CO_2	Reducing
Be-O_2	Berthierine	O_2	Oxidizing

[a] Composition presented in Equation (1).
[b] Composition from Amouric and Parron (1985).
[c] Composition presented in Equation (2).

transfer reactions (Table 1), until a gas phase begins to form or until the primary mineral completely dissolves. Dissolution of glauconite or berthierine (composition from Fu et al., 2015) releases different species into the pore water, such as $Fe^{3+}_{(aq)}$, $Fe^{2+}_{(aq)}$, $Mg^{2+}_{(aq)}$, and $H_4SiO_{4(aq)}$ (Eqs. (1) and (2)). Therefore, this would lead to a supersaturation with respect to different secondary minerals, and, consequently, allows their precipitation. All minerals that are included in the thermodynamic database of the computer code PhreeqcI ("phreeqc.dat"; Partkhurst and Appelo, 2013) can newly form, provided that they reach saturation, for instance, calcite, dolomite, magnesite, siderite, berthierine, chrysotile, chlorite with a basal spacing of 7Å (chlorite7A taken from the database "wateq4f.dat"; Parkhurst and Appelo, 2013), kaolinite, and $Fe(OH)_{3(a)}$. Chalcedony (cryptocrystalline $SiO_{2(s)}$) is considered as the reactive solid $SiO_{2(s)}$ phase to newly form in the model instead of quartz. This is because formation of secondary $SiO_{2(s)}$ in form of small crystals or as overgrowth was proven as one product of glauconite alteration in the Siri field (Fu, 2014; Fu et al., 2015). Quartz formation from aqueous solutions, which are supersaturated with respect to quartz, is a sluggish reaction, whereas less stable $SiO_{2(s)}$ minerals (e.g., chalcedony or cristobalite) commonly control dissolved silica concentrations (Appelo and Postma, 1994).

$$K_{0.489}Na_{0.045}Mg_{0.281}Al_{1.387}Fe_{1.183}Si_{3.327}O_{10}(OH)_{2(Glauconite)}$$
$$+ 10H_2O \leftrightarrow 0.489K^+ + 0.045Na^+ + 0.281Mg^{2+}$$
$$+ 1.387Al(OH)_4^- + 1.069Fe^{3+} + 0.114Fe^{2+} + 3.327H_4SiO_4$$
$$+ 3.144OH^-$$

$$(1)$$

$$Fe_{1.634}Mg_{0.328}Al_{1.324}Si_{1.526}O_5(OH)_{4(Berthierine)}$$
$$+ 7.896H^+ \leftrightarrow 1.634Fe^{2+} + 0.328Mg^{2+} + 1.324Al^{3+}$$
$$+ 1.526H_4SiO_4 + 2.896H_2O$$

$$(2)$$
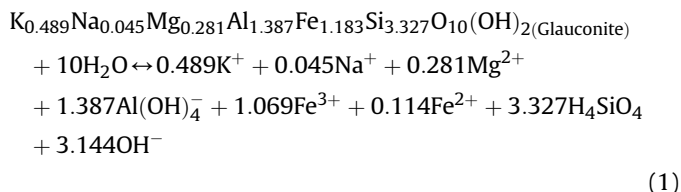
Hydrogeochemical modeling was carried out by using the computer code PhreeqcI (Parkhurst and Appelo, 2013). The database "phreeqc.dat" of PhreeqcI (Parkhurst and Appelo, 2013) was applied for calculating the species distribution of equilibrium among pore water, minerals and gas. The equilibrium constants and their temperature-pressure dependence for the chemical reactions

of all involved aqueous species, minerals and gas components are defined in this database except for glauconite, berthierine, magnesite, chlorite7A. The thermodynamic data of magnesite and chlorite7A were taken from the database "wateq4f.dat" of PhreeqcI (Parkhurst and Appelo, 2013). The predictive approach for estimating the thermodynamic data of phyllosilicates (Vieillard and Mathieu 2009; Vieillard et al., 2011, and references therein) was used to calculate the thermodynamic data of glauconite and berthierine. These data (for details, see Appendix A) were defined in the input file. PhreeqcI calculates the pressure dependence of the equilibrium constants of minerals by using the molar volume of these minerals (Parkhurst and Appelo, 2013).

Addition of different reactants in a series of modeling scenarios leads to a board range of pH-E_H conditions in the modeling reactor in which glauconite or berthierine is present as the single primary mineral (Table 1). An alternative scenario Gl2-CO_2 + CH_4 uses a glauconite which composition is provided by Amouric and Parron (1985; labeled as glauconite2; $K_{0.709}Na_{0.084}Ca_{0.043}(Al_{0.427-}Fe^{3+}_{0.869}Fe^{2+}_{0.176}Mg_{0.521})(Si_{3.793}Al_{0.207})O_{10}(OH)_2)$; for its thermodynamic data, see Appendix A). Such scenarios, on the one hand, shall identify the pH-E_H conditions of glauconite dissolution as well as of berthierine formation and dissolution, and, on the other hand, determine the CO_2-sequestering capacity of glauconite and the factors influencing this capacity.

3. Modeling results

3.1. Scenario Gl-CO_2

Addition of CO_2 into the reactor triggers a decrease in pH of the pore water (from 5.8 down to 3.2 in Fig. 1). This leads to release of $Fe^{3+}_{(aq)}$ species into the pore water, and, consequently, to oxidizing conditions prevailing in the pore water (Figs. 1 and B.1; rH > 24; rH = 2 (pH + pe); E_H from 293 to 614 mV; logarithm of oxygen fugacity: log $f(O_{2(g)})$ from −20 to −14). The calculated E_H increases with increasing addition of CO_2 and reaches 614 mV at the final reaction step (Table 2; Fig. B.1). Less than 0.15 mmol glauconite dissolves in 1.0 L of a 1.5 molal NaCl solution, even when a very low pH of 3.2 and a high pCO_2 of 230 atm are achieved at the final reaction step (Figs. 1 and B.1). This indicates that only small amounts of glauconite dissolve in order to establish its solubility
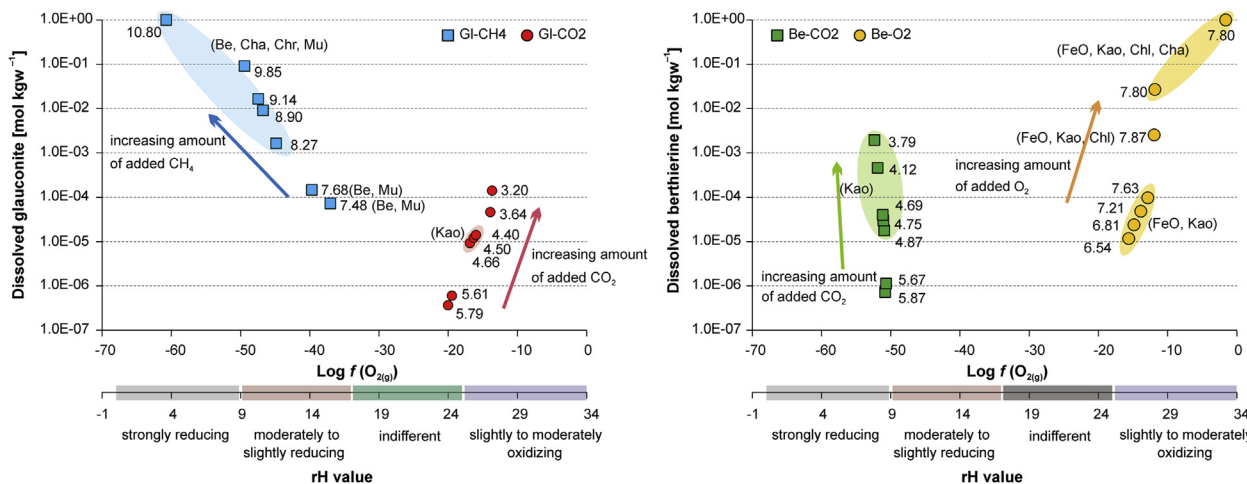
Figure 1. Calculated mass conversion of glauconite or berthierine and main hydrogeochemical parameters resulting from increasing addition of CH_4, CO_2 or O_2 as function of log $f(O_{2(g)})$ and rH value in scenarios Gl-CH_4, Cl−CO_2, Be−CO_2, and Be−O_2 (reaction steps 1–10). $f(O_{2(g)})$: fugacity of molecular oxygen; rH value: characterizing redox-conditions in combination of pH and pe values; rH = 2 (pe + pH); colored bars: classification of redox-conditions in terms of rH value according to Hölting and Coldewey (2005); numbers next to symbols: calculated pH of pore water; abbreviations in brackets: minerals newly formed at the different reactions steps; Be: berthierine; Cha: chalcedony; Chr: chrysotile; Chl: chlorite7A; FeO: $Fe(OH)_{3(a)}$; Kao: kaolinite; Mu: muscovite.

Table 2
Main hydrogeochemical parameter values (including CO_2-trappling capacity) calculated for selected scenarios at the final reaction step.

	Added reactants	pH	Redox- conditions			Primary mineral assemblage	Dissolved glauconite (mol per kg pore water)	Products	Amount of secondary carbonates (mol per kg pore water)			
			Log $f(O_2)$	rH[a]	E_H (mV)				Cc	Do	Ma	Si
Gl-CO_2 + CH_4	CO_2, CH_4	5.52	−57.9	5.1	−177	Glauconite[b]	1.0	Be, Cha, Mu, Ma,			0.04	
Gl2-CO_2 + CH_4	CO_2, CH_4	5.85	−58.1	4.9	−200	Glauconite2[c]	1.0	Be, Cha, Do, Ma, Si		0.07	0.30	0.26
Gl-CO_2	CO_2	3.20	−13.7	27.2	614	Glauconite	1.4×10^{-4}					
Siri-ODP-siderite[d]	CO_2, CH_4, H_2	7.03	−59.6	4.2	−292	Siri field	0.76	Be, Cc, Cha, Mu, Kao, Si	1.06			0.42

Be: berthierine; Cc: calcite; Cha: chalcedony; Do: dolomite; Kao: kaolinite; Ma: magnesite; Mu: muscovite; Si: siderite; Blanks indicate that no secondary mineral forms.
[a] rH = 2 (pe + pH) according to Hölting and Coldewey (2005).
[b] Composition presented in Equation (1).
[c] Composition from Amouric and Parron (1985).
[d] Scenario taken from Fu et al. (2015): the primary mineral assemblage of the Siri oilfield plus 1 wt.-% goethite.

equilibrium −in other words, glauconite remains stable under oxidizing conditions− in spite of such a low pH. In consequence, no potential secondary mineral achieves saturation except for kaolinite which forms with negligible amounts during the reaction steps 3 to 5 (Figs. 1 and B.1).

3.2. Scenarios Gl-CH_4, Gl-CO_2 + CH_4 and Gl2-CO_2 + CH_4

In contrast, glauconite can be regarded as a highly soluble mineral under reducing conditions which are established by continuous addition of CH_4 in scenario Gl-CH_4 (Table 1). With ongoing addition of CH_4, the calculated log $f(O_{2(g)})$ and the calculated rH constantly decrease to −61 and to 3.6 at the final reaction step, respectively (Fig. 1). The pre-assigned 1.0 mol of primary glauconite is completely dissolved by the CH_4 addition of 0.13363 mol (Figs. 1 and 2). In parallel, berthierine, chalcedony, chrysotile, and muscovite form at the expense of glauconite (Fig. 2). This reductive transformation of glauconite to these secondary

minerals is accompanied by an increase in the calculated pH of the pore water (up to 10.8; Figs. 1 and 2).

The calculated results of scenario Gl-CH_4 show that glauconite can completely dissolve under reducing conditions. Consequently, an alternative scenario (Gl-CO_2 + CH_4) was calculated to test whether glauconitic sandstones, which provide electrons for glauconite dissolution, could act as an efficient rock matrix for CO_2 sequestration. To simulate this situation, CO_2 is gradually added into the pore water together with CH_4, until 1.0 mol of glauconite is completely dissolved. In this scenario, CH_4 is generically considered as one of potential electron donors (e.g., degradable, methane-producing organic matter), which exist in the glauconitic sandstones or which are co-injected with CO_2, in order to create reducing conditions and to drive reductive dissolution of glauconite.

The calculated diagenetic features of scenario Gl-CO_2 + CH_4 resemble the results of scenario Gl-CH_4: complete glauconite dissolution is associated with precipitation of berthierine,
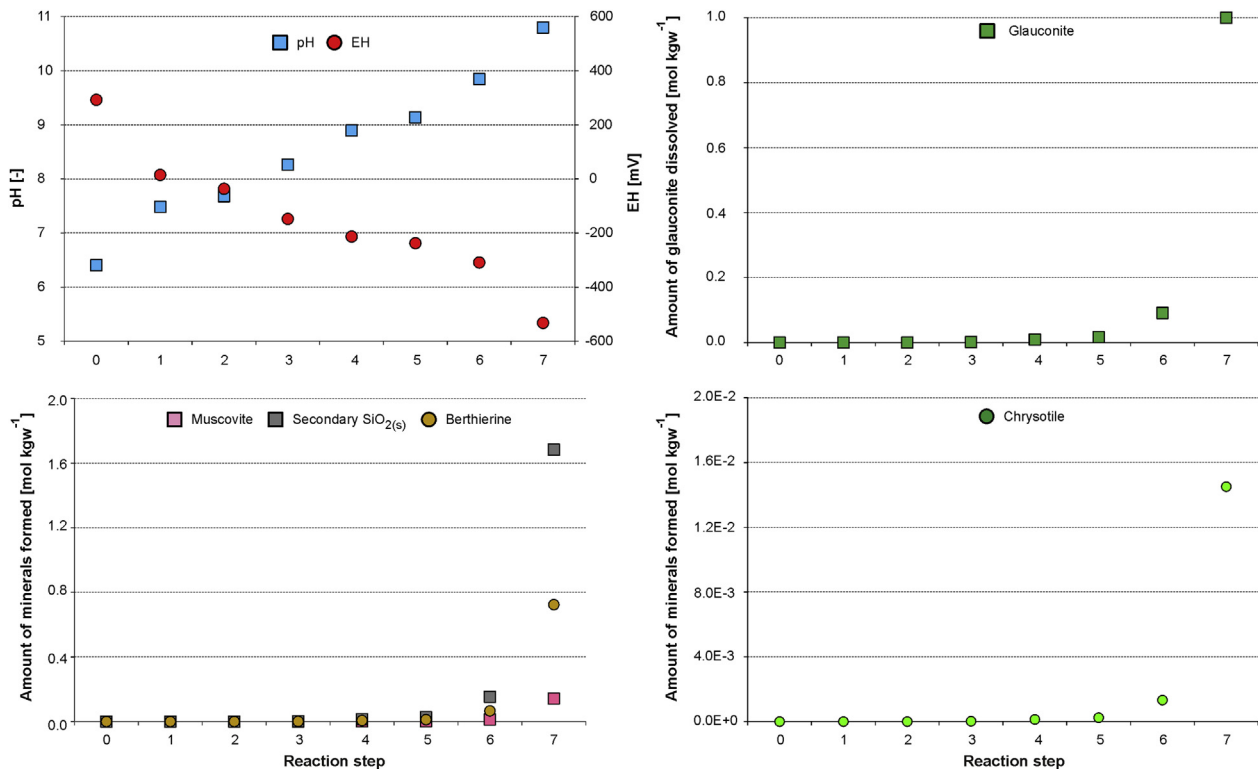
Figure 2. Calculated results of modeling scenario Gl-CH_4 with increasing addition of CH_4 into pore water (reaction steps 0–7). Amount of CH_4 incrementally added: 0.00001, 0.00001, 0.0002, 0.001, 0.001, 0.01, and 0.12141 mol per reaction step.

chalcedony, and muscovite (Fig. B.2). In addition, only 0.04 mol of magnesite forms, when 1.0 mol of glauconite is completely dissolved (Table 2; Fig. B.2). This implies a very limited CO_2-sequestering capacity of the glauconite in the Siri oilfield in form of carbonate precipitation.

Scenario Gl2-CO_2 + CH_4 considers glauconite2 (composition according to Amouric and Parron, 1985) in order to test whether the chemical composition of glauconite affects the fate and behavior of CO_2. Glauconite2 contains more Fe and Mg, but is depleted in Al compared to the glauconite in the Siri field. Less available Al in glauconite2 leads to a reduced formation of berthierine in scenario Gl2-CO_2 + CH_4 (0.5 mol kgw^{-1} berthierine in Fig. B.3) when compared to scenario Gl-CO_2 + CH_4 (0.7 mol kgw^{-1} berthierine in Fig. B.2). Therefore, more Fe- and Mg-species, which are not bound in berthierine, are removed from the pore water by formation of Fe- and Mg-bearing carbonates in scenario Gl2-CO_2 + CH_4 (Table 2; Fig. B.3). In consequence, the glauconite2 affords a slightly higher CO_2-sequestering capacity compared to the glauconite from the Siri field when exposed to reducing conditions (Table 2).

3.3. Scenarios Be–CO_2 and Be–O_2

The calculated results of scenario Gl-CH_4 show that berthierine newly forms at the expense of glauconite under reducing conditions. The question still remains open whether the newly formed berthierine can subsequently dissolve and be transformed to Fe- and/or Mg-bearing carbonates under specific pH-E_H-pCO_2 conditions. If so, this transformation would allow a further removal of gaseous and/or aqueous CO_2 in glauconitic sandstones. This was tested by calculating two additional scenarios Be–CO_2 and Be–O_2 to identify the pH-E_H conditions of berthierine dissolution and its potential secondary minerals. Both scenarios consider 1.0 mol of berthierine in each reactor. The pore water of these two generic reactors undergoes stepwise addition of CO_2 and O_2, respectively, in order to create a broad range of pH-E_H conditions.

Addition of CO_2 into the pore water equilibrating with berthierine leads to the release of aqueous Fe^{2+} species. Thus, reducing conditions prevail within the reactor (scenario Be–CO_2; rH < 8.6 and log $f(O_{2(g)})$ < −50 in Figure 1; E_H < 7 mV in Fig. B.4). Although the pH of the pore water decreases to 3.8 and the $pCO_{2(g)}$ increases to 230 atm due to CO_2 addition, less than 2.0 mmol of berthierine dissolve in 1.0 L of pore water to reach its solubility equilibrium (Figs. 1 and B.4). In other words, berthierine remains stable under reducing conditions, even at a low pH. In parallel, trace amounts of kaolinite form at the expense of berthierine (1.3 mmol kgw^{-1} at the final step in Fig. B.4), whereas formation of any Fe- and/or Mg-bearing carbonate is prevented.

On the contrary, addition of O_2 leads to oxidizing conditions in the pore water (scenario Be–O_2; rH > 26 and log $f(O_{2(g)})$ > −50 in Figure 1; E_H > 360 mV in Fig. B.5). Berthierine gets unstable during stepwise addition of O_2 (Fig. B.5), as proposed by Rivard et al. (2013). An increase in pH is accompanied by weak berthierine dissolution and, finally, the calculated pH reaches 7.8 at maximum (Figs. 1 and B.5). At the final reaction step, the pre-assigned primary berthierine is completely converted to kaolinite, $Fe(OH)_{3(a)}$, chlorite7A, and secondary $SiO_{2(s)}$ under oxidizing conditions (Figs. 1 and B.5).

4. Discussion and implications

Several studies (see Section 1) considered deep glauconitic sandstones as suitable CO_2 storage sites. They suggested that the actual processes includes glauconite dissolution and carbonate formation (especially of siderite), because glauconite is rich in Fe and Mg. Our modeling results reveal that in view of thermodynamics injection of pure CO_2 (without any additional reducing agent) into glauconitic sandstones, which are free of any degradable organic matter or other electron-donors, is incapable of inducing formation of Fe- and/or Mg-bearing carbonates with relevant amounts. The reason for this is that injection of pure CO_2 into glauconitic sandstones leads to mild acidic and oxidizing conditions under which glauconite remains stable due to its low aqueous solubility and under which formation of any secondary carbonate is prevented (scenario Gl-CO_2; Table 2). On the contrary, glauconite can completely dissolve under reducing conditions, provided that sufficient electron donors are available (scenario Gl-CH_4). There are several natural sites of such glauconitic sandstones, for instance, the Nullawarre Greensand with incorporated organic lamellae and bone fragments (Boyd et al., 2004) or the Siri oilfield after oil charging. Alternatively, reducing agents (such as CH_4) have to be co-injected with CO_2 in order to establish reducing conditions in glauconitic environments. Even under reducing conditions, sandstones with a glauconite, which chemical composition resembles the composition of the glauconite in the Siri field, have a limited CO_2-sequestering capacity due to only trace amounts of carbonates newly formed (scenario Gl-CO_2 + CH_4; Table 2). The reason is that berthierine acts as a "great attractor" due to its low solubility constant, and, therefore, is the ultimate sink for aqueous Fe^{2+}, Mg^{2+}, Al^{3+}, and H_4SiO_4 species released by glauconite dissolution. Therefore, our modeling results demonstrate that a replacement of glauconite by annite (e.g., Gunter et al., 1997, 2000) and calculations excluding berthierine formation are incapable of correctly predicting the CO_2-sequestering capacity in glauconitic environments. Apart from berthierine, secondary $SiO_{2(s)}$ and potassium mica would concurrently form at the expense of glauconite. As one of the most important products of glauconite dissolution, berthierine remains stable over a broad pH range under reducing conditions. Even at a high $pCO_{2(g)}$, transformation of berthierine to carbonates is prevented under reducing conditions (scenario Be–CO_2). In contrast, strong dissolution of berthierine can be activated only by a sufficient supply with oxidants. Concurrently, it will be transformed to secondary $SiO_{2(s)}$, chrysotile, $Fe(OH)_{3(a)}$, and kaolinite (scenario Be–O_2).

The CO_2-sequestering capacity is limited by berthierine formation in glauconitic sandstones under reducing conditions. Nevertheless, several factors can enhance the CO_2-sequestering capacity of glauconitic sandstones: an appropriate chemical composition of glauconite, and the overall mineralogical composition of glauconite-bearing sandstones (Table 2). Sandstones containing a glauconite with a composition similar to $K_{0.489}Na_{0.045}Mg_{0.281}Al_{1.387}Fe_{1.183}Si_{3.327}O_{10}(OH)_2$ (e.g., measured in the Siri field by Fu, 2014) are unsuitable for CO_2 sequestration via glauconite dissolution and the resulting carbonate formation (scenario Gl-CO_2 + CH_4; Table 2). In comparison, glauconite with higher contents of Fe, Mg and Ca has a much higher CO_2-sequestering capacity via carbonate precipitation under reducing conditions (scenario Gl2-CO_2 + CH_4; Table 2). It can be expected that the Ca:Fe:Mg ratio in glauconite could also affect the CO_2-sequestering potential of glauconite, as different carbonates are characterized by individual solubility constants under the same temperature-pressure conditions.

Table 2 includes the results of scenario Siri-ODP-siderite which simulates the alteration of the glauconitic reservoir rocks of the Siri field due to oil degradation (for details, see Fu et al., 2015). Compared to scenario Gl-CO_2 + CH_4, glauconite with a same composition dominates in the mineral assemblage of scenario Siri-ODP-siderite which additionally includes albite, K-feldspar, anorthite, muscovite, and goethite as primary minerals (4.0, 4.0, 2.0, 1.0, and 1.0 wt.%, respectively). In the presence of water, aqueous hydrocarbons are unstable and can be gradually degraded to CO_2, CH_4,

and H_2 (Seewald, 2003). Correspondingly, reducing conditions also prevail in scenario Siri-ODP-siderite. Thus, both scenarios, Gl-CO_2 + CH_4 and Siri-ODP-siderite, have comparable pH-E_H conditions at the starting conditions. In the case of less glauconite dissolution in scenario Siri-ODP-siderite, higher amounts of carbonates (calcite and siderite) are precipitated due to dissolution of anorthite and goethite, when compared with scenario Gl-CO_2 + CH_4 (Table 2). This comparison shows that the CO_2-trapping capacity in glauconitic sandstones noticeably depends on the primary mineral assemblage of glauconitic sandstones, for instance, can be enhanced via carbonate precipitation due to anorthite and/or goethite abundance in the mineral assemblage (Table 2).

5. Conclusions

Under elevated temperature-pressure conditions (78 °C and 230 atm in the model), CO_2-induced acid attack on glauconite drives the evolution of acidic and oxidizing conditions in aqueous solutions. The reason for this is that glauconite-derived $Fe^{3+}_{(aq)}$-species are released into the pore water in absence of electron donors (e.g., degradable and sedimentary organic matter, crude oil, natural gas or co-injected methane). Under these acidic and oxidizing conditions, only trace amounts of glauconite can dissolve and carbonate formation is prevented. Electron transfer to ferric iron bound in glauconite is the key pre-requisite for its intense dissolution (reductive dissolution). Reductive dissolution of glauconite releases Fe^{2+}, Mg^{2+}, Al^{3+}, and H_4SiO_4 species into pore water. Due to the low solubility of berthierine, berthierine formation strongly fixes Fe^{2+}- and Mg^{2+}-cations so that they are no longer available for carbonate formation. Such reductive dissolution of glauconite and the resulting berthierine formation should be commonly accompanied by formation of secondary $SiO_{2(s)}$ and potassium mica. Although berthierine formation inhibits or strongly limits CO_2 sequestration via carbonate precipitation in glauconitic sandstones, in general, the case-specific chemical composition of glauconite affects the mass conversion of newly formed carbonates, and, consequently, the CO_2-sequestering capacity. In addition, the overall mineralogical composition of the rock matrix also affects the amount of authigenic carbonates. While calcite formation and the thereby caused CO_2 sequestration result from acid buffering reactions between the injected CO_2 and anorthite, siderite formation is triggered by the reductive (and acidic) dissolution of Fe(III)-oxide-hydroxide.

Injection of CO_2 in glauconitic or other sandstones is integrated in a complex reaction web. Thus, instead of modeling approaches limited to selected reactions of interest, hydrogeochemical modeling approaches considering a complex web of interconnected reactions must be used to correctly predict the final fate of injected CO_2 and the actual sequestering capacity via mineral precipitation. Our modeling results reveal that among other factors (1) the presence of electron donors (e.g., degradable and sedimentary organic matter, crude oil or natural gas), (2) the co-injection of methane or alternative reducing agents, (3) the availability of Ca-plagioclase, (4) the appropriate chemical composition of glauconite relatively rich in Mg, Fe, and Ca, and (5) the presence of goethite as a product of former, oxic glauconite alteration enhance CO_2 sequestration in glauconitic environments via carbonate formation to different degrees.

Besides its geochemical control on CO_2 sequestration, berthierine formation may change the physical properties of oil-/gas reservoir rocks (e.g., decrease of permeability). Berthierine remains stable under reducing conditions due to its low aqueous solubility. Once formed, the relevant mass conversion of berthierine exclusively via acidic dissolution is negligible under typical reservoir conditions. This indicates that it is almost impossible to remove

berthierine by technical measures such as acidification of formation water (without addition of any electron acceptor) in order to enhance the near-wellbore porosity/permeability properties of oil reservoirs. However, berthierine could dissolve under oxidizing conditions, but this is only a more or less theoretical, and non-realistic technical measure for oil reservoirs.

Appendix A. Supplementary data

Supplementary data related to this article can be found at http://dx.doi.org/10.1016/j.marpetgeo.2015.01.008.

References

Amouric, M., Parron, C., 1985. Structure and growth mechanism of glauconite as seen by high resolution transmission electron microscopy. Clays Clay Minerals 33, 473—482.

Appelo, C.A.J., Postma, D., 1994. Geochemistry, Groundwater and Pollution. A.A. Balkema, Rotterdam, pp. 213—214.

Bacon, D.H., Murphy, E.M., 2011. Managing chemistry underground: is co-sequestration an option in selected formations? Energy Procedia 4, 4457—4464.

Boyd, G.A., Wallace, M.W., Holdgate, G.R., Gallagher, S.J., 2004. Marine clays and porosity evolution in the Nullawarre Greensand, Otway Basin, southeastern Australia. In: PESA Eastern Australasian Basins Symposium II Held in Adelaide, 20-22 September, 2004.

Fu, Y., van Berk, W., Schulz, H.-M., 2012. Hydrogeochemical modelling of fluid—rock interactions triggered by seawater injection into oil reservoirs: case study Miller field (UK North Sea). Appl. Geochem. 27, 1266—1277.

Fu, Y., van Berk, W., Schulz, H.-M., 2013. Temporal and spatial development of scale formation: one-dimensional hydrogeochemical transport modeling. J. Pet. Sci. Eng. 112, 273—283.

Fu, Y., 2014. Development and Application of Numerical Modeling for Evaluating and Predicting Hydrogeochemical Processes Temporally and Spatially Evolving in Petroleum Reservoirs (Ph.D. thesis). In: Case Studies: Miller Oilfield (UK North Sea) and Siri Oilfield (Danish North Sea). 73—75. Clausthal University of Technology, Germany, p. 111.

Fu, Y., van Berk, W., Schulz, H.-M., Mu, N., 2015. Berthierine formation in reservoir rocks from the Siri oilfield (Danish North Sea) as result of fluid-rock interactions: part II. Deciphering organic-inorganic processes by hydrogeochemical modeling. Mar. Pet. Geol. 65, 317—326. http://dx.doi.org/10.1016/j.marpetgeo.2015.01.007.

Gaus, I., Azaroual, M., Czernichowski-Lauriol, I., 2005. Reactive transport modelling of the impact of CO_2 injection on the clayey cap rock at Sleipner (North Sea). Chem. Geol. 217, 319—337.

Gunter, W.D., Wiwchar, B., Perkins, E.H., 1997. Aquifer disposal of CO_2-rich greenhouse gases: extension of the time scale of experiment for CO_2-sequestering reactions by geochemical modelling. Mineral. Petrol. 59, 121—140.

Gunter, W.D., Perkins, E.H., Hutcheon, I., 2000. Aquifer disposal of acid gases: modelling of water—rock reactions for trapping of acid wastes. Appl. Geochem. 15, 1085—1095.

Hölting, B., Coldewey, W.G., 2005. Hydrogeologie: Einführung in die Allgemeine und Angewandte Hydrogeologie, 6. Auflage. Spektrum, Akademischer Verlag, p. 150 (in German).

Humez, P., Audigane, P., Lions, J., Chiaberge, C., Bellenfant, G., 2011. Modeling of CO_2 leakage up through an abandoned well from deep saline aquifer to shallow fresh groundwaters. Transp. Porous Media 90, 153—181.

Kumar, A., Noh, M., Pope, G.A., Sepehrnoori, K., Bryant, S., Lake, L.W., 2004. Reservoir simulation of CO_2 storage in deep saline aquifer. In: SPE 89343, Presented at the 2004 SPE/DOE Fourteenth Symposium on Improved Oil Recovery Held in Tulsa, Oklahoma, USA, 17-21 April, 2004.

Mackenzie, K.J.D., Cardile, C.M., Brown, I.W.M., 1988. Thermal and mössbauer studies of iron-containing hydrous silicates, VII. Glauconite. Thermochem. Acta 136, 247—261.

Parkhurst, D.L., Appelo, C.A.J., 2013. Description of Input and Examples for PHREEQC Version 3 — a Computer Program for Speciation, Batch-reaction, One-dimensional Transport, and Inverse Geochemical Calculations (Chapter A43). In: U.S. Geological Survey Techniques and Methods Book 6. Available only at: http://pubs.usgs.gov/tm/06/a43/.

Pruess, K., Garcia, J., Kovscek, T., Oldenburg, C., Rutqvist, J., Steefel, C., Xu, T., 2002. Intercomparison of Numerical Simulation Codes for Geologic Disposal of CO_2. Technical report Lawrence Berkeley Laboratory report, LBNL-51813.

Rivard, C., Pelletier, M., Michau, N., Razafitianamaharavo, A., Bihannic, I., Abdelmoula, M., Ghanbaja, J., Villiéras, F., 2013. Berthierine-like mineral formation and stability during the interaction of kaolinite with metallic iron at 90 °C under anoxic and oxic conditions. Am. Mineral. 98, 163—180.

Seewald, J.S., 2003. Organic-inorganic interactions in petroleum producing sedimentary basins. Nature 426, 327—333.

Sheldon, N.D., Retallack, G.J., 2002. Low oxygen levels in earliest Triassic soils. Geology 30, 919—922.

Stokkendal, J., Friis, H., Svendsen, J.B., Poulsen, M.L.K., Hamberg, L., 2009. Predictive permeability variations in a Hermod sand reservoir, stine segments, Siri Field, Danish North Sea. Mar. Pet. Geol. 26, 397—415.

Vieillard, P., Mathieu, R., 2009. A predictive model for the enthalpies of hydration of zeolites. Am. Mineral. 94, 565—577.

Vieillard, P., Blanc, P., Fialips, C.I., Gailhanou, H., Gaboreau, S., 2011. Hydration thermodynamics of the SWy-1 montmorillonite saturated with alkali and alkaline-earth cations: a predictive model. Geochim. Cosmochim. Acta 75, 5664—5685.

Xu, T., Apps, J.A., Pruess, K., 2004. Numerical simulation of CO_2 disposal by mineral trapping in deep aquifers. Appl. Geochem. 19, 917—936.